Influence of Gyroscopic Effects on Nonlinear Dynamics of High-Speed Planetary Gears Having an Elastic Ring

Chenxin Wang and Robert G. Parker
Department of Mechanical Engineering, University of Utah, Salt Lake City, UT 84112, USA

Summary. Numerical simulations show that gyroscopic effects can significantly influence the nonlinear dynamics (resonances and parametric instabilities) of planetary gears having a deformable ring at high speed. Analytical solutions at resonances and parametric instabilities that include the gyroscopic effects are derived and used to explain the numerical results.

Introduction

Vibrations of planetary gears arise primarily from periodically changing sun-planet and ring-planet tooth mesh excitation as the gears rotate. A resonance occurs when a harmonic L of the mesh frequency Ω_{m} approaches a natural frequency ω_q (i.e., $L\Omega_{\mathrm{m}} \approx \omega_q$). A parametric instability occurs when $L\Omega_{\mathrm{m}} \approx \omega_p + \omega_q$, where ω_p and ω_q can be the same. Near resonances or parametric instabilities, vibrations can become large enough that nonlinear tooth separation occurs. The ring has substantial elastic deformation when it is designed to be thin for weight saving. Gyroscopic (i.e., Coriolis) effects become significant for high-speed systems, but their influence on the nonlinear dynamics of planetary gears having an elastic ring are not yet known.

This work derives closed-form solutions for the nonlinear dynamics of planetary gears with a deformable ring using the model in [1]. The model includes speed-dependent gyroscopic and centripetal effects. The tooth mesh excitation is modeled as time-varying stiffnesses that include tooth separation nonlinearity. Numerical integration of the dynamic model shows the significant impact of gyroscopic effects on the resonances and parametric instabilities at high speed.

Numerical results

Fig. 1 shows the RMS of dynamic ring-planet mesh deflection from numerical integration of a planetary gear system having a deformable ring without (black dashed line) and with (green dotted line) gyroscopic effects. The differences highlight the significant influence of gyroscopic effects. One resonance ($\Omega_{\mathrm{m}} \approx \omega_4$) and one parametric instability ($\Omega_{\mathrm{m}} \approx \omega_1 + \omega_2$) are present for the system without gyroscopic effects. When gyroscopic effects are included, an additional resonance at $\Omega_{\mathrm{m}} \approx \omega_3$ occurs. For the resonance $\Omega_{\mathrm{m}} \approx \omega_4$, the peak amplitude decreases and the peak resonant frequency shifts to the right with inclusion of gyroscopic effects. The parametric instability $\Omega_{\mathrm{m}} \approx \omega_1 + \omega_2$ is absent for the system with gyroscopic effects.

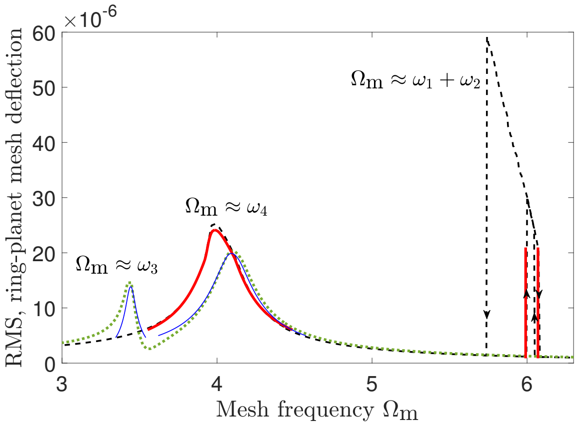

Figure 1: RMS (mean removed) values of dimensionless ring-planet mesh deflection from numerical integration of a planetary gear system having a deformable ring without (black dashed line) and with (green dotted line) gyroscopic effects over a range of dimensionless mesh frequencies. These RMS results are identical for every planet. The arrows indicate results from increasing and decreasing speed simulations. The thick (red) and thin (blue) solid lines are the analytical results from Eq. (1) for the two resonances $\Omega_{\mathrm{m}} \approx \omega_3$ and $\Omega_{\mathrm{m}} \approx \omega_4$ and Eq. (3) for the one parametric instability $\Omega_{\mathrm{m}} \approx \omega_1 + \omega_2$ for the system without and with gyroscopic effects.

Analytical explanation

Resonances

The amplitude-frequency relation for a resonance $L\Omega_{\mathrm{m}} \approx \omega_q$ (whether the system is gyroscopic or not) is derived as

$$\Omega_{\mathrm{m}} = \frac{\omega_q}{L} + \frac{\omega_q}{La_q}\left(2R_1 + R_2 a_q \pm \sqrt{4|R_3|^2 - (\nu_q a_q)^2}\right), \tag{1a}$$

$$R_3 = N\left(k_{\mathrm{s}1}^{(L)} \bar{\Delta}_{\mathrm{s}1}^{[q]} \Delta_{\mathrm{s},0} + k_{\mathrm{r}1}^{(L)} \bar{\Delta}_{\mathrm{r}1}^{[q]} \Delta_{\mathrm{r},0}\right), \tag{1b}$$

where a_q is the real-valued amplitude of the resonant mode, ν_q is the modal damping ratio, R_1 and R_2 are real-valued terms associated with tooth contact loss, N is the number of planets, $k_{j1}^{(L)}$ for $j = \mathrm{s}, \mathrm{r}$ are the L-th harmonic coefficients (complex-valued) of the first sun-planet and ring-planet mesh stiffness variations, $\Delta_{j,0}$ are the static sun-planet and ring-planet mesh deflections (real-valued and identical for every planet) due to the applied torque, $\Delta_{j1}^{[q]}$ are the first sun-planet and ring-planet modal mesh deflections (complex-valued), and the overbar denotes complex conjugate. Vanishing of the square root term in Eq. (1a) gives the peak resonant amplitude

$$a_{q,\mathrm{p}} = 2|R_3|/\nu_q. \tag{2}$$

Eqs. (1b) and (2) explain why the resonance $\Omega_\mathrm{m} \approx \omega_3$ does not occur for the system without gyroscopic effects but occurs for the system with them (Fig. 1). In the absence of gyroscopic effects, mode 3 is a mode where the modal sun-planet and ring-planet mesh deflections vanish (i.e., $\Delta_{\mathrm{s}n}^{[3]} = \Delta_{\mathrm{r}n}^{[3]} = 0$ for $n = 1, 2, \ldots, N$) [2], such that the R_3 for this mode and the peak amplitude $a_{3,\mathrm{p}}$ in Eq. (2) vanish. When gyroscopic effects are included, mode 3 becomes a mode with nonzero $\Delta_{\mathrm{s}n}^{[3]}$ and $\Delta_{\mathrm{r}n}^{[3]}$ [3]. This leads to nonzero R_3 in Eq. (1b) and nonzero $a_{3,\mathrm{p}}$ in Eq. (2) and therefore the occurrence of the resonance $\Omega_\mathrm{m} \approx \omega_3$ for the system with gyroscopic effects in Fig. 1.

Eq. (1) shows that gyroscopic effects shift the resonant frequencies by changing the natural frequencies. The ω_4 increases when gyroscopic effects are included, so the resonant frequency for $\Omega_\mathrm{m} \approx \omega_4$ shifts to the right. This prediction matches the numerical results in Fig. 1.

Eqs. (1b) and (2) reveal that gyroscopic effects affect the peak amplitudes of resonances by changing vibration mode quantities. Gyroscopic effects change the modal mesh deflections $\Delta_{\mathrm{s}n}^{[4]}$ and $\Delta_{\mathrm{r}n}^{[4]}$. At high speed, this change is significant. This alters the values of R_3 in Eq. (1b). R_3 changes significantly for mode 4, which affects the associated peak amplitude $a_{4,\mathrm{p}}$. As shown in Fig. 1, the analytical predictions capture this effect.

Parametric instabilities

The boundaries of the range of mesh frequencies for a parametric instability $L\Omega_\mathrm{m} \approx \omega_p + \omega_q$ to occur are derived as

$$\Omega_\mathrm{m}^{\{L,p,q\}} = \frac{(\omega_p + \omega_q)}{L} \pm \frac{\nu_p\omega_p + \nu_q\omega_q}{L}\sqrt{|D_{pq}^{(L)}|^2/(\nu_p\nu_q) - 1}, \tag{3a}$$

$$D_{pq}^{(L)} = N(k_{\mathrm{r}1}^{(L)}\bar{\Delta}_{\mathrm{r}1}^{[p]}\bar{\Delta}_{\mathrm{r}1}^{[q]} + k_{\mathrm{s}1}^{(L)}\bar{\Delta}_{\mathrm{s}1}^{[p]}\bar{\Delta}_{\mathrm{s}1}^{[q]}). \tag{3b}$$

Eq. (3a) gives that a parametric instability is eliminated by damping when

$$|D_{pq}^{(L)}| < \sqrt{\nu_p\nu_q}. \tag{4}$$

Eqs. (3) and (4) apply to both non-gyroscopic and gyroscopic planetary gears having a deformable ring.

Eqs. (3b) and (4) show that gyroscopic effects change the occurrence of a parametric instability by changing modal mesh deflections. The parametric instability $\Omega_\mathrm{m} \approx \omega_1 + \omega_2$ for the system without gyroscopic effects has $|D_{1,2}^{(1)}| = 0.0211 > \sqrt{\nu_1\nu_2} = 0.02$. Therefore, this parametric instability is present in Fig. 1. When gyroscopic effects are included, the modal mesh deflections $\Delta_{j1}^{[1]}$ and $\Delta_{j1}^{[2]}$ for $j = \mathrm{s}, \mathrm{r}$ change so that $|D_{1,2}^{(1)}|$ decreases (see Eq. (3b)). This leads to $|D_{1,2}^{(1)}| = 0.0172 < \sqrt{\nu_1\nu_2} = 0.02$. The parametric instability $\Omega_\mathrm{m} \approx \omega_1 + \omega_2$ is absent in Fig. 1 in the presence of gyroscopic effects.

Conclusions

Gyroscopic effects alter the occurrence of resonances, shift resonant frequencies, and change resonant amplitudes associated with nonlinear behavior induced by contact loss. These influences are significant for high-speed planetary gears having an elastic ring. A closed-form amplitude-frequency relation derived for the resonances of planetary gears without and with gyroscopic effects reveal how these effects change the resonant behavior by their influence on the natural frequencies and vibration modes. For example, changes of modal mesh deflections of a resonant mode can change the resonant amplitude and, sometimes, change whether a resonance occurs or not.

The influence of gyroscopic effects on parametric instabilities of planetary gears having an elastic ring is similarly substantial. The analytical results reveal that gyroscopic effects change the occurrence/absence of parametric instabilities and the mesh frequency range where a given instability occurs. These effects arise principally from changes to the modal mesh deflections of the participating modes.

References

[1] Wang C., Parker R.G. (2020) Dynamic modeling and mesh phasing-based spectral analysis of quasi-static deformations of spinning planetary gears with a deformable ring. *Mechanical Systems and Signal Processing* **136**:106497.

[2] Wu X., Parker R.G. (2008) Modal properties of planetary gears with an elastic continuum ring gear. *Journal of Applied Mechanics, Transactions ASME* **75**:0310141–03101412.

[3] Wang C., Parker R.G. (2021) Modal properties and parametrically excited vibrations of spinning epicyclic/planetary gears with a deformable ring. *Journal of Sound and Vibration* **494**:115828.